Action of nicotine and analogs on acetylcholine receptors having mutations of transmitter-binding site residue αG153

Snehal Jadey, Prasad Purohit, and Anthony Auerbach

Department of Physiology and Biophysics, State University of New York, Buffalo, NY 14214

A primary target for nicotine is the acetylcholine receptor channel (AChR). Some of the ability of nicotine to activate differentially AChR subtypes has been traced to a transmitter-binding site amino acid that is glycine in lower affinity and lysine in higher affinity AChRs. We studied the effects of mutations of this residue (αG153) in neuromuscular AChRs activated by nicotine and eight other agonists including nornicotine and anabasine. All of the mutations increased the unliganded gating equilibrium constant. The affinity of the resting receptor (K_d) and the net binding energy from the agonist for gating (ΔG_B) were estimated by cross-concentration fitting of single-channel currents. In all but one of the agonist/mutant combinations there was a moderate decrease in K_d and essentially no change in ΔG_B. The exceptional case was nicotine plus lysine, which showed a large, >8,000-fold decrease in K_d but no change in ΔG_B. The extraordinary specificity of this combination leads us to speculate that AChRs with a lysine at position αG153 may be exposed to a nicotine-like compound in vivo.

The Journal of General Physiology

INTRODUCTION

Acetylcholine (ACh) receptor channels (AChRs) are ligand-gated ion channels that regulate the flow of cations across cell membranes. These membrane proteins alternatively adopt two stable shapes having a closed or an open channel (C↔O). In the periphery, AChRs mediate vertebrate neuromuscular synaptic transmission, and in the central nervous system, they are thought to play roles in cognition, attention, addiction, analgesia, and other behaviors (Gotti et al., 1997; Lindstrom, 1997; Changeux and Edelstein, 2001). Neuronal AChRs are sites of action for nicotine and are potential targets for the treatment of schizophrenia, Alzheimer's, epilepsy, and other human neurological diseases (Jensen et al., 2005; Gotti et al., 2006).

AChRs spontaneously switch between C and O conformations, but without agonists, the unliganded "gating" equilibrium constant is small and there is hardly any constitutive activity. The rate and probability of adopting the O shape increase substantially when the transmitter-binding sites are occupied by certain ligands, such as the neurotransmitter ACh. In neuromuscular AChRs, many other ligands including nicotine and choline increase the open-channel probability (P_o) but to smaller maximum extents than ACh does.

The neuromuscular AChR (adult-type) has two transmitter-binding sites located in the extracellular domain at the α–ε- and α–δ-subunit interfaces (Fig. 1 A). A thermodynamic cycle provides a good description of AChR activation (Fig. S1) (Monod et al., 1965; Karlin, 1967; Auerbach, 2012). The unliganded gating equilibrium constant (E_0, which sets the minimum P_o) is determined by the intrinsic energy difference between the O and C conformational ensembles with only water present at the transmitter-binding sites (ΔG_0). When agonists are present, a low-to-high affinity change at each site generates binding energy (ΔG_B) that increases the relative stability of O and, hence, P_o. The maximum P_o is determined by the energy difference between O versus C when agonists are present at both transmitter-binding sites (ΔG_2). From the cycle, and with equivalent binding sites (Jha and Auerbach, 2010),

$$\Delta G_2 = 2\Delta G_B + \Delta G_0. \quad (1)$$

In AChRs, ΔG_0 = +8.4 kcal/mol ($P_o^{min} \sim 10^{-6}$), ΔG_2^{ACh} = −1.9 kcal/mol ($P_o^{max} \sim 0.96$), and ΔG_B^{ACh} = −5.1 kcal/mol (Nayak et al., 2012).

Three aromatic rings in the α-subunit side of each binding site provide most of the ΔG_B energy for gating with ACh: αW149 (in loop B), and αY190 and αY198 (both in loop C; Fig. 1 B) (Purohit et al., 2012). In this paper, we examine in detail the functional properties of αG153 (also called GlyB2), a loop B residue that is near this "aromatic triad." We investigated the effects of αG153 mutations on ΔG_0, ΔG_B (with several agonists), and the lower affinity equilibrium dissociation constant for agonist binding to resting AChRs (K_d).

Correspondence to Anthony Auerbach: auerbach@buffalo.edu

Abbreviations used in this paper: ACh, acetylcholine; AChBP, ACh-binding protein; AChR, ACh receptor channel; CCh, carbamylcholine.

The Rockefeller University Press $30.00
J. Gen. Physiol. Vol. 141 No. 1 95–104
www.jgp.org/cgi/doi/10.1085/jgp.201210896

There are three reasons why we chose to focus our attention on αG153. First, some neuronal AChR subtypes (those with α_2, α_3, α_4, and α_6 subunits) have a lysine at this position. These subtypes have a higher affinity for nicotine than for ACh (Connolly et al., 1992; Chavez-Noriega et al., 1997), and a lysine mutation of αG153 in α_7 or α_1 AChRs increases the resting affinity for nicotine (Corringer et al., 1998; Grutter et al., 2003; Xiu et al., 2009). A search of the sequence database shows that in vertebrate α subunits, the αG153 residue is usually a glycine (61%), sometimes a lysine (38%), and rarely anything else.

Second, whereas almost all mutations of amino acids at the binding sites decrease activation by agonists, in neuromuscular AChRs, those of αG153 increase activation. The αG153 mutations that have been studied so far increase activity by making ΔG_0 less positive and decreasing K_d, for both ACh and its breakdown product choline (Zhou et al., 1999; Purohit and Auerbach, 2011). The αG153S mutation causes a human congenital myasthenic syndrome as a result of these two effects (Sine et al., 1995). We wanted to ascertain the generality of the uniquely positive effect on AChR activation of αG153 mutations.

The third reason we probed αG153 in detail was to explore its role in the agonist-binding structural rearrangement. The targeting of a receptor by a ligand depends on K_d. Evidence was presented recently suggesting that the binding of ligands to resting AChRs requires both diffusion and a conformational change that involves, in part, a "capping" motion of loop C (Jadey and Auerbach, 2012). This is an interesting development because it offers a novel mechanism for ligands to modulate transmitter occupancy of the binding sites, for example by altering noncompetitively the intrinsic equilibrium constant of the binding conformational change. Other experiments show that the rate constants for association and dissociation of choline to the transmitter-binding sites have a high temperature dependence in the mutant αG153S (Gupta and Auerbach, 2011). This suggests that this residue, which is in loop B, is involved in the binding conformational change.

In this paper, we present binding and gating constants, determined by single-channel kinetic analyses, for nicotine, nornicotine, and anabasine in WT neuromuscular AChRs. We also give the parameters for these and six additional agonists in AChRs having a mutation of αG153 (Fig. 1 C). The results show that all αG153

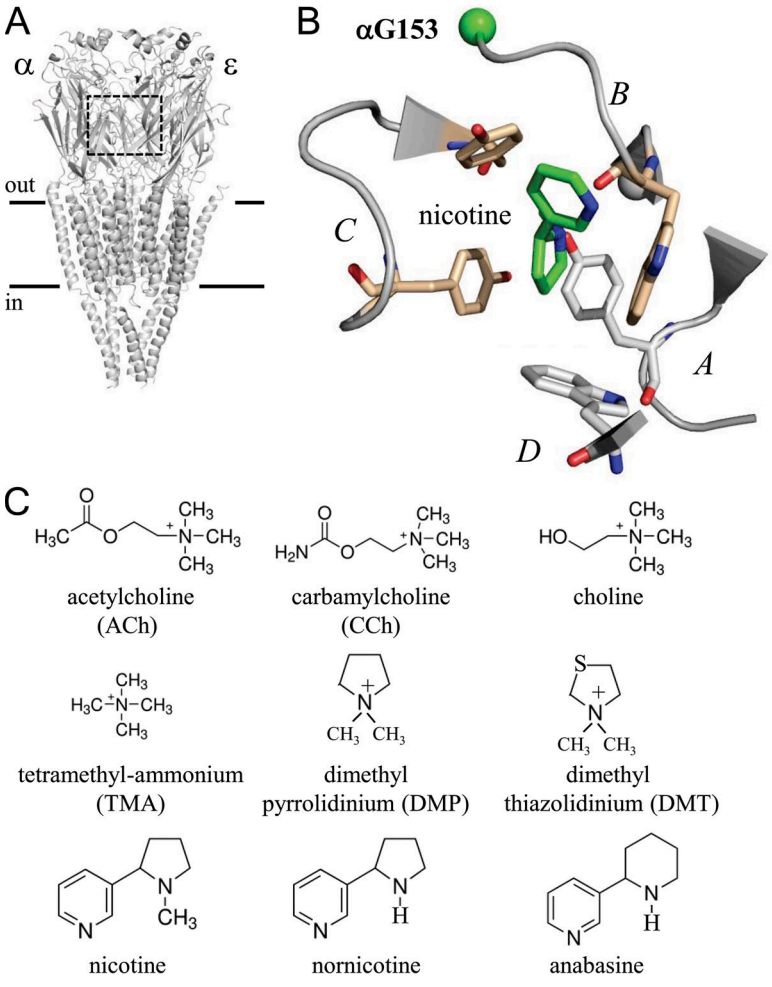

Figure 1. Structures. (A) Low resolution cryo-EM image of the unliganded *Torpedo* AChR (Protein Data Bank accession no. 2bg9) (Unwin, 2005). A transmitter-binding site region is boxed. Lines mark approximately the membrane. (B) Close-up of a ligand-binding site of the *Lymnaea* ACh–binding protein (Protein Data Bank accession no. 1uw6) (Rucktooa et al., 2009), a homologue of the AChR transmitter-binding site. Loops A–D are labeled. Cα of αG153 (mouse numbering) is a green sphere, nicotine is green, and the aromatic triad is tan. (C) Structures of the agonists.

mutations increase unliganded gating, and that all agonist/mutant combinations increase resting affinity but have little effect on the affinity ratio. The increase in resting affinity is particularly great in the lysine plus nicotine combination. In the ACh-binding protein (AChBP), a good structural model for the AChR transmitter-binding site (Brejc et al., 2001), the residue corresponding to αG153 is a serine or a glycine. However, no structures of AChBPs with a lysine (or other side chains) at this position have yet been reported.

MATERIALS AND METHODS

Mutagenesis and expression

The QuikChange Site-Directed Mutagenesis kit (Agilent Technologies) was used to make mutant cDNAs of mouse AChR subunits. All sequences were verified by dideoxy sequencing. Transient transfection of HEK 293 cells was performed using calcium phosphate precipitation. 3.5 µg of subunit cDNA was added in the ratio 2:1:1:1 (α1, β, δ, and ε) to each 35-mm culture dish of cells. Cells were incubated for ∼16 h at 37°C and were then washed with fresh media. Electrophysiological recordings were performed ∼20 h after transfection.

Single-channel recording

Single-channel recordings were from cell-attached patches at 23°C. The bath solution was (mM): 142 KCl, 5.4 NaCl, 1.8 $CaCl_2$, 1.7 $MgCl_2$, and 1 HEPES, pH 7.4. The pipette solution contained the specified concentration of agonist dissolved in Dulbecco's PBS (mM): 137 NaCl, 0.9 $CaCl_2$, 0.5 $MgCl_2$, 1.5 KH_2PO_4, and 8.1 $NaHPO_4$, pH 7.4. Unless noted otherwise, the cell membrane potential (V_m) was +100 mV so that the currents were in the outward direction. For details see Jadey et al. (2011).

Equilibrium and rate constant estimation

The equilibrium dissociation constant of resting receptors ($K_d = k_{off}/k_{on}$) and the diliganded gating equilibrium constant ($E_2 = f_2/b_2$) were estimated by fitting globally interval durations obtained at several different agonist concentrations by:

$$\begin{matrix} & 2[A]k_{on} & & [A]k_{on} & & f_2 & \\ 2A+C & \leftrightarrow & A+AC & \leftrightarrow & A_2C & \leftrightarrow & A_2O \\ & k_{off} & & 2k_{off} & & b_2 & \end{matrix}$$

(SCHEME 1)

where [A] is the agonist concentration, C is a resting (low affinity/closed-channel) AChR, and O is an active (high affinity/open-channel) AChR. The model assumes that the two binding sites are functionally equivalent (see Fig. S1). $E_2 = f_2/b_2$ and $\Delta G_2 = -0.59 \ln E_2$. See the first section of the Results for a discussion of how brief, undetected gating intermediate states do not influence the ΔG_B estimates obtained by using Scheme 1 and Eq. 1.

The equilibrium dissociation constant for channel block by the agonist (K_B) was estimated by fitting the single-channel current amplitudes by $(i/i_0) = 1/(1 + [A]/K_B)$, where i is the amplitude at concentration [A], and i_0 is the current amplitude extrapolated to zero concentration. This equation is an approximation that assumes b_2 is much slower in blocked versus unblocked receptors.

E_0 estimation

For E_0 measurements, the αG153 (GlyB2) mutants were coexpressed with a gain-of-function double mutant construct εL269F (in M2) + βT456F (in M4) + δ^{WT}, and single-channel currents were recorded without any agonists in the pipette or bath. The effects of the background mutations on ΔG_0 were shown experimentally to be approximately independent (Jadey et al., 2011). Individually, each of these mutations increases E_2 by an approximately equivalent increase in E_0: εL269F by 179-fold (Jha et al., 2009) and βT456F by 5.2-fold (Mitra et al., 2004). Thus, the double mutant background combination increases E_0 (and, hence, E_2) by ∼930-fold ($\Delta\Delta G_0 = -4.0$ kcal/mol). The observed E_0 for each αG153 mutant was therefore corrected as observed $E_0^{mut}/930$.

For a few mutants, the spontaneous unliganded open- and closed-interval durations within clusters were well described by a single-exponential component. For these, f_0 and b_0 were simply the inverse mean lifetimes of the nonconducting and conducting intervals. Most of the αG153 mutants produced unliganded currents exhibiting multiple open/shut components within clusters (Purohit and Auerbach, 2009). For these, the intra-cluster–interval durations were fitted by using a kinetic model having the appropriate number of nonconducting (three) and conducting (two) states. The f_0 and b_0 were the inverse lifetimes of the predominant shut and open components.

Dose–response analysis

The probability of being open within a cluster (P_o) was calculated as $f_2/(f_2 + b_2)$. f_2 was estimated from the high concentration asymptote of the effective opening rate constant (the inverse of the longest component of intra-cluster closed-interval durations, f*), and b_2 was the closing rate constant measured at a low agonist concentration where there was no apparent channel block. This P_o corresponds to a whole-cell current measurement with rapid agonist application (no desensitization). The EC_{50} was estimated as the concentration producing a half-maximal response. Each symbol is the average P_o from more than three patches.

E_2 estimation

E_2 measurements for the various side-chain/agonist combinations were made at +100 mV and by using previously characterized background mutations that decreased E_0 (made ΔG_0 less positive) but had no effect on ΔG_B (Table S8). The change in membrane potential from −100 to +100 mV, which reverses the direction of current flow, decreases E_0 by a factor of 12.5 ($\Delta\Delta G_0$ = +1.5 kcal/mol) but has no effect on ΔG_B. The backgrounds were necessary to compensate for the higher E_0 (less positive ΔG_0) of some of the αG153 mutations. The mutated side chains of the background constructs were shown by experiments to be approximately energetically independent (Jadey et al., 2011), except for αV261F, which was assumed to be independent of the other perturbations. The observed gating rate constants f_2 and b_2 were corrected for the effects of the background. The reported ΔG_B values were calculated using the background-corrected values of ΔG_0 (notation, background in parentheses; αG153 side chain/agonist): (a: εS450W), S/Cho, A/Cho, P/Cho, K/Cho; (b: δI43H + εS450W), S/DMP, S/DMT, S/Nic, S/TMA, S/CCh, P/DMP, P/DMT, P/Nic, A/DMP, A/DMT, A/Nic, K/DMP, K/DMT; (c: αT422V + δI43H + εS450W), S/ACh; (d: αT422V + δI43A + εS450W), P/TMA, P/CCh, P/ACh, A/TMA, A/CCh, A/ACh; (e: αV261F + δI43A + εS450W), K/Nic, K/TMA, K/CCh; (f: αV261F + δI43A + εS450W + εI257A), K/ACh (all at +100 mV). The fold changes in f_2/b_2 (WT/mut) for backgrounds are (notation, background; αG153 side chain/agonist): +200-mV depolarization, 0.7/8.3; a, 1.5/0.12; b, 0.068/1.2; c, 0.015/6.5; d, 0.095/8.2; e, 0.00087/1.54; f, 0.000077/8.0. The corresponding equilibrium values (fold change in $E_0/\Delta\Delta G_0$ in kcal/mol) are: +200-mV depolarization, 0.08/−1.5; a, 12.5/+1.5; b, 0.057/+1.7; c, 0.0023/+3.6; d, 0.0116/+2.6; e, 0.00056/+4.4; f, 0.0000096/+6.8.

Online supplemental material

The supplemental material consists of eight supplemental tables that give all of the primary and background-corrected rate and

equilibrium constants. There are two supplemental figures. Fig. S1 shows the thermodynamic cycle of AChR activation. Fig. S2 shows examples of nicotine-activated single-channel currents in various αG153 mutants, and the corresponding shut- and open-interval duration histograms. The online supplemental material is available at http://www.jgp.org/cgi/content/full/jgp.201210896/DC1.

RESULTS

Gating models and protein engineering

The isomerization of an AChR is a huge chemical reaction that involves energy (structure) changes of many elements in the protein–lipid–water complex. It is a priori certain that within the global conformational change the system adopts transiently short-lived (ps-μs) intermediate states in its passage between the stable C and O ground states. In experiments, three such intermediates have been detected indirectly by using rate-equilibrium analyses, and one intermediate has been detected directly by using high resolution kinetic analyses.

Here, we use the word "gating" to describe the complete allosteric transition between the C and O end states, rather than just the microscopic event that regulates ion and water passage across the membrane. The state model for gating can be expanded to incorporate the intermediate states. Assuming that there is a single sequential pathway through the intermediates, $C \leftrightarrow O$ becomes $C \leftrightarrow F^1 \leftrightarrow F^2 \leftrightarrow ... O$, where each F represents an intermediate state. In our experiments, the F states were too brief to be detected; hence, the ΔG_B values we obtained by using a two-state gating scheme reflect the sum of the energy changes for all of the steps in the sequence. Although the affinity change appears to occur early in the sequence, the ΔG_B measurements we report pertain to the total energy arising from the affinity change, regardless of when it occurs in the gating sequence.

Some agonist/mutant combinations are difficult to study using WT AChRs because the gating rate and equilibrium constants are outside of the range suitable for single-channel cluster analysis, which is approximately $\Delta G_2 = \pm 2$ kcal/mol ($0.03 < E_2 < 30$). We addressed this problem by adding voltage and background mutations that increased or decreased ΔG_0 to known extents. These manipulations placed ΔG_2 and, hence, the rate and equilibrium constants into a more easily measurable range (Eq. 1). Previous studies showed that none of the background perturbations we used had any effect on ΔG_B (Jadey et al., 2011). We corrected the observed ΔG_2 value by the ΔG_0 offset provided by the background to estimate gating parameters for our reference condition (−100 mV; WT ΔG_0). The magnitudes of the background effects on ΔG_0 are given at the end of Materials and methods.

We use interchangeably the gating energy and equilibrium constant: ΔG (kcal/mol) = −0.59lnE. The error limits on the rate and equilibrium constants are given

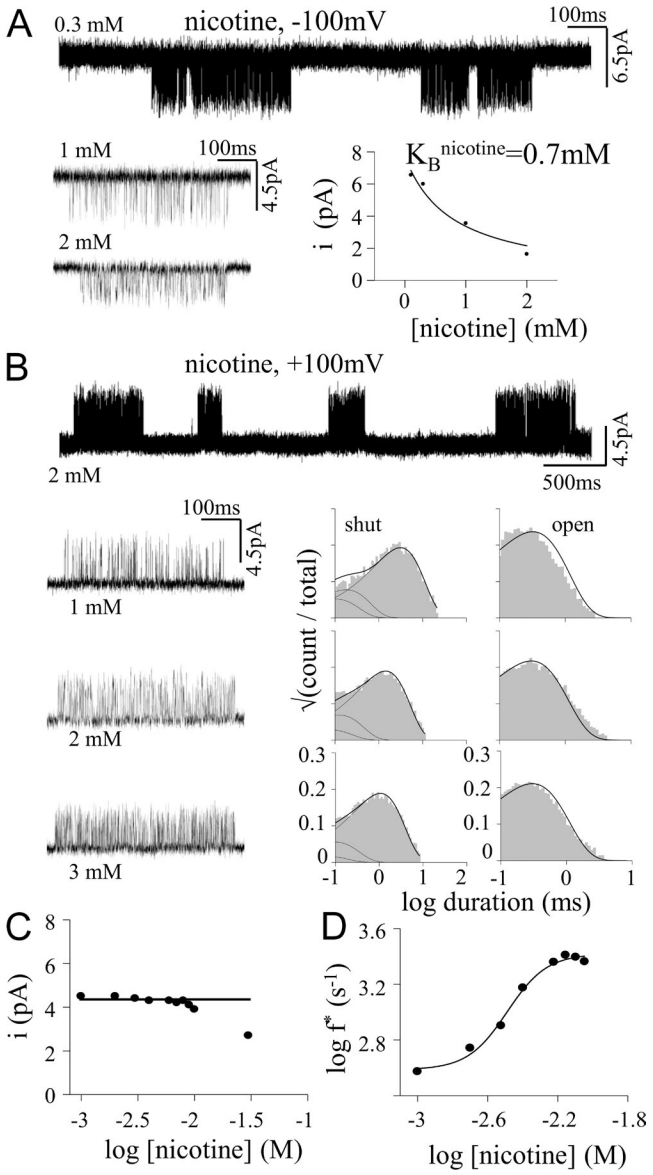

Figure 2. Action of nicotine on WT AChRs. (A; top) Low time-resolution view of single-channel current clusters, each reflecting the activity of an individual AChR (open is down). (Bottom left) Higher time-resolution view of clusters. (Bottom right) The current amplitude (i) declines with increasing concentration because nicotine is a fast channel blocker. $K_B^{nicotine}$ is the equilibrium dissociation constant of nicotine for the pore. (B; top) Low time-resolution view of current clusters (open is up). (Bottom) Clusters of openings at increasing [nicotine] and corresponding intra-cluster–interval duration histograms. Solid lines are the global fit by Scheme 1. (C) Single-channel current amplitude at 100 mV is constant at [nicotine] < ∼10 mM because depolarization reduces channel block. (D) With increasing [nicotine], the effective opening rate (f*) reaches a plateau that is the fully liganded opening rate constant (∼2,400 s^{-1}). The highest tested concentration was 8 mM nicotine. The E_2 estimates were not affected by channel block because the transmitter-binding sites are fully saturated at ∼6 mM. The activation constants for nicotine on WT AChRs (−100 mV) are $E_2 = 0.87$, $K_d = 1$ mM, and $\Delta G_B = -4.1$ kcal/mol (Table S1).

in Table S8. A 20% difference in an equilibrium constant translates to an ∼0.1 kcal/mol difference in energy. The error limits on the energy values are approximately ±0.2 kcal/mol.

Nicotine, nornicotine, and anabasine in WT AChRs

Nicotine, one of the drugs in tobacco that is addictive, is consumed daily by more than one billion people worldwide. The action of nicotine on neuromuscular AChRs has been investigated (Akk and Auerbach, 1999), but new technical advances in rate constant estimation motivated us to revisit this agonist. Fig. 2 A shows single-channel currents from adult WT mouse neuromuscular AChRs activated by nicotine at a membrane potential of −100 mV. The top trace is a low time-resolution view showing that openings (down) occurred in clusters. The events within clusters reflect multiple cycles of agonist binding and channel gating in a single AChR, and the intervening silent periods reflect times when all of the AChRs in the patch are in states associated with desensitization. This clustering allows the estimation of binding and gating rate constants for single AChRs. It was not possible to use neuronal AChRs in our experiments because their single-channel openings are not clustered. The higher resolution single-channel traces show that in WT neuromuscular AChRs, millimolar concentrations of nicotine are required to elicit clusters having a moderately high P_o.

With increasing concentrations of nicotine, the single-channel current amplitude declined because this agonist is a fast channel blocker (Fig. 2 A, bottom right). From the pattern of decline we estimate that nicotine has an equilibrium dissociation constant for the pore of $K_B^{nicotine}$ = 0.7 mM. Channel block by nicotine not only limits cellular currents at high concentrations but, because we must fully saturate the binding sites to measure the diliganded gating equilibrium constant E_2, also our ability to estimate K_d and E_2.

To estimate these quantities, we depolarized the membrane to reduce channel block and reverse the direction of the ionic current. This allowed us to use higher [nicotine] (Fig. 2, B and C; open is up). Under these conditions, outward single-channel currents could be measured using [nicotine] up to ∼10 mM, which is sufficiently high to saturate the two AChR transmitter-binding sites (Fig. 2 D). The net effect of +200-mV depolarization (and the current reversal) is to increase ΔG_0 by approximately +1.5 kcal/mol (Nayak et al., 2012). We added a background mutation that canceled the effects of depolarization on gating (that decreased ΔG_0 by approximately −1.5 kcal/mol), so the equilibrium and rate constants we measured at +100 mV pertain to our reference condition, which is WT AChRs at −100 mV (Jadey et al., 2011). From the durations of open and shut intervals within clusters, measured at several different [nicotine], we estimate that at the reference condition $K_d^{nicotine}$ = 1.0 mM and the diliganded gating equilibrium constant $E_2^{nicotine}$ = 0.87 (ΔG_2 = −0.08 kcal/mol). This E_2 estimate is ∼1.7 times greater than the one reported previously (Akk and Auerbach, 1999), presumably because in those experiments channel block prevented the use of saturating [nicotine].

The WT unliganded gating equilibrium constant is $E_0^{WT} = 7 \times 10^{-7}$ or ΔG_0 = +8.4 kcal/mol (Nayak et al., 2012). The average energy from the affinity change for each nicotine molecule can be calculated by using Eq. 1: $2\Delta G_B^{nicotine}$ = (−0.08–8.4) kcal/mol. We calculate that in adult WT neuromuscular AChRs, each nicotine molecule provides on average $\Delta G_B^{nicotine}$ = −4.1 kcal/mol to power channel opening, which is only ∼1 kcal/mol more positive than with ACh (ΔG_B^{ACh} = −5.1 kcal/mol) (Jadey et al., 2011). A 1-kcal/mol loss of favorable (more negative) binding energy at each of the two binding sites translates to an ∼30-fold reduction in E_2 and a reduction in the maximum P_o from ∼0.97 to ∼0.48. Nicotine is a moderately effective partial agonist of neuromuscular AChRs (Table S1).

We also investigated at the single-channel level two related tobacco alkaloids, anabasine and nornicotine (Kem et al., 1997; Papke et al., 2007). Another ligand, methyl-anabasine, blocked the channel so avidly that depolarization to +100 mV was insufficient to allow binding site saturation and rate constant estimation.

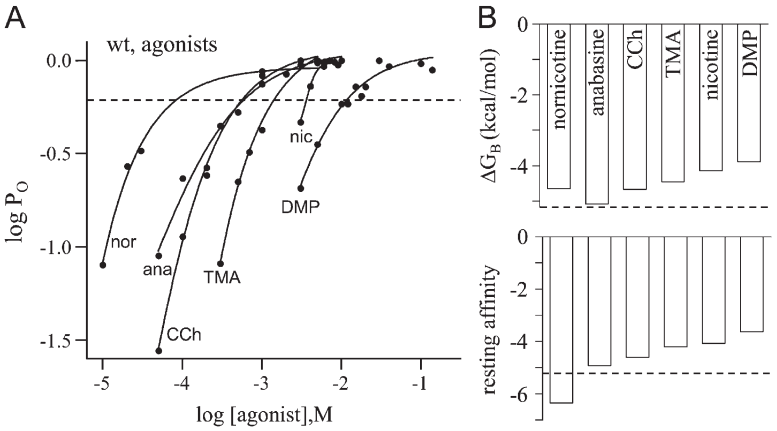

Figure 3. Dose–response curves and activation constants for agonists in WT AChRs. (A) Normalized intra-cluster open probability (P_o) as a function of [agonist]. EC_{50} (dashed line) was smallest for nornicotine and largest for DMP (Table S4). (B) Activation constants determined by cross-concentration fitting of single-channel current-interval durations. Dashed line, ACh value. (Top) Binding energy from the agonist for gating (ΔG_B). (Bottom) Resting affinity on a log scale ($-0.59\ln(1/K_d)$). Nornicotine has almost the same resting affinity and binding energy as ACh.

As with nicotine, we measured single-channel currents at different agonist concentrations to estimate E_2 and calculate K_d from the ratio of the dissociation/association rate constant estimates obtained by cross-concentration fitting. To summarize the results graphically, we also estimated the cluster P_o at each concentration and fit these values to an empirical equation to generate a normalized dose–response curve (Fig. 3 A). The E_2^{WT} values (which depend only on ΔG_B and determine the maximum P_o) for nicotine, nornicotine, and anabasine were, respectively, 0.87, 5.0, and 21 (Fig. 3 B, top, and Table S1). Anabasine provides almost as much binding energy as the neurotransmitter. The order of K_d values for these three agonists was nornicotine (21 µM) < anabasine (230 µM) < nicotine (1,000 µM). The differences in K_d were mainly attributable to changes in the agonist association rate constant. The activation equilibrium constants for all of the ligands shown in Fig. 1 C in adult WT neuromuscular mouse AChRs have been estimated (Table S2) (Jadey et al., 2011).

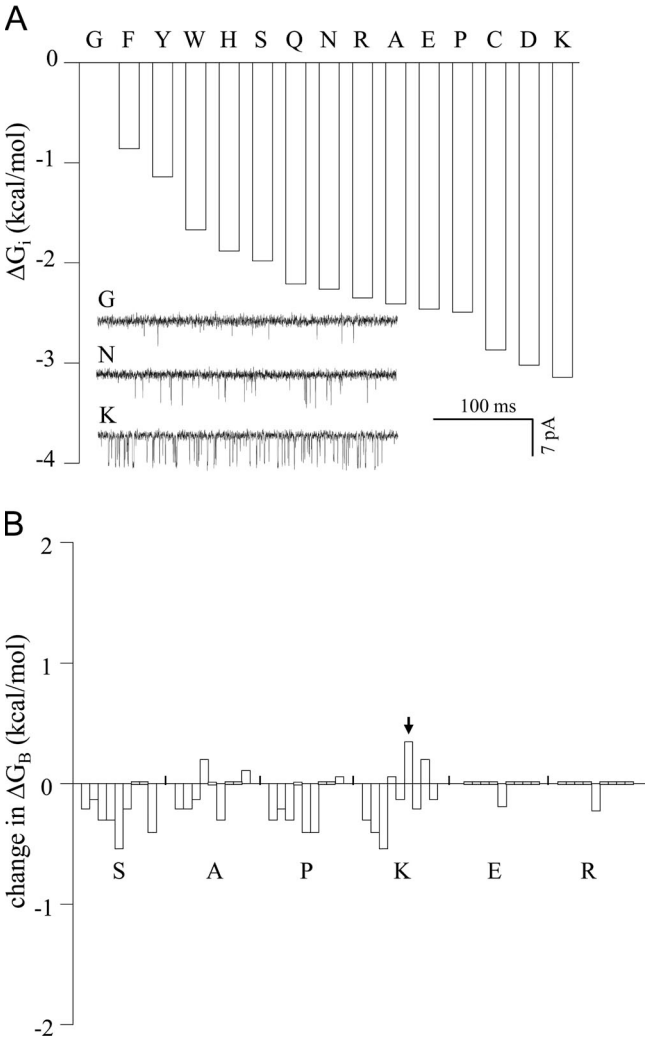

Figure 4. The unliganded gating equilibrium constant and affinity ratio in αG153 mutants. (A) Bars show the fold change in E_0 relative to the WT value (7×10^{-7}) on a log scale (ΔG_0). All mutations increased E_0, with lysine having the largest effect (200-fold) (Table S3). (Inset) Example currents obtained in the absence of agonists (V_m = −100 mV; open is down; background, εL269F + βT456I). (B) None of the mutations had a large effect on ΔG_B for any agonist (Table S5). Agonist order for αG153K is (left to right): choline, DMP, DMT, TMA, ACh, nicotine (arrow), CCh, anabasine, and nornicotine.

αG153 mutants: Unliganded gating and the affinity ratio

The analysis of αG153 mutations on AChR activation starts with describing their effects on the intrinsic, unliganded gating equilibrium constant E_0. In many places in the protein, side-chain substitutions alter the relative stability of the O versus C ground states and, hence, E_0 and dose–response profiles. The logarithm of the fold change in E_0 (relative to the WT) is proportional to the change in the intrinsic energy of the unliganded C↔O gating isomerization (ΔG_0). We first sought to estimate ΔG_0 values for different mutations of αG153.

Some example currents (obtained in the absence of any agonists) and ΔG_0 values for 14 different αG153 mutations are shown in Fig. 4 A. All of the mutations increased E_0 (increased the relative stability of O; ΔG_0 is more negative) (Table S3). The large aromatic substitutions F, Y, W, and H had relatively small effects (less than −2 kcal/mol), but those of C, D, and K substitutions were greater (approximately −3 kcal/mol). We could not discern a clear pattern relating side-chain chemistry with ΔG_0, so perhaps this energy is mainly determined by the disposition of the loop B backbone. Of the mutations we studied, E_0 was smallest with glycine and largest with lysine, the two amino acids that are present naturally in AChRs. The higher E_0 value of αG153K AChRs will cause higher leak currents and stronger cellular responses (lower EC_{50} and higher maximum P_o values) for all agonists (Table S4) (Zhou et al., 1999).

Next, we determined the effects of αG153 mutations on ΔG_B, which is the energy for increasing P_o by agonists arising from the low-to-high affinity change at the binding site. We examined all 9 agonists and 6 side chains (GSAPKER) in 39 different combinations. The results are summarized in Fig. 4 B.

The effects of αG153 mutations on ΔG_B were, in all cases, small. The largest increase in the agonist energy was only −0.5 kcal/mol, and the largest decrease was only +0.3 kcal/mol (Table S5). These energies are miniscule compared with the ∼2-kcal/mol changes in ΔG_B apparent with some mutations of the aromatic triad (Purohit et al., 2012). For the side-chain/agonist combinations we tested, αG153 had little to do with setting the energy from the agonist for gating.

aG153 mutants: Dose–response curves and K_d

Fig. 5 A shows dose–response curves for six different αG153 mutants using nicotine as the agonist. All of the αG153 mutations increased the resting affinity (reduced

K_d) for nicotine (Fig. 5 B and Table S6). The increase with E, R, P, A, and S substitutions was similar and modest, on average ~20-fold (approximately −1.8 kcal/mol). In all cases, the decrease in K_d was mainly caused by an increase in the agonist association rate constant.

The effect of the lysine mutation was, however, remarkable. This substitution increased the affinity of the resting binding site for nicotine by 8,130-fold (−5.3 kcal/mol), from ~1 mM to ~120 nM. As a consequence of both this extraordinarily large decrease in K_d and the increase in E_0 caused by the lysine substitution, the EC_{50} of the normalized dose–response curve for nicotine shifted from 1.3 mM in the WT to 724 nM in αG153K (Table S4). At [nicotine] generating approximately equivalent cluster P_o values, the single-channel currents in all of the αG153 constructs were similar (Fig. 5 B, bottom).

Because of the unusual effect of the lysine substitution on activation by nicotine, we examined the dose–response properties of other agonists using this mutant (Fig. 6). The resting affinity was highest for nicotine, but those for nornicotine and carbamylcholine (CCh), too, were high (K_d = 325 and 700 nM) (Table S7).

Fig. 7 shows the change in the resting affinity relative to the WT for 21 different αG153 mutant/agonist combinations, on a log scale. Most of these combinations behaved similarly, with the side-chain substitution increasing the resting affinity for the agonist by ~25-fold (−1.9 kcal/mol) (Table S6). The only extraordinary effect was for the nicotine plus lysine combination, described above. A smaller, but notable, effect was for the CCh plus lysine combination, in which K_d^{CCh} decreased by 580-fold (−3.8 kcal/mol).

DISCUSSION

Nicotine, nornicotine, and anabasine on WT AChRs

Because so many people consume tobacco, nicotine and nornicotine can be considered to be physiological ligands, along with ACh and its metabolites choline and betaine. It is currently not possible to measure from single channels the binding, gating, and blocking constants (energies) for these agonists in neuronal AChRs. Although there is substantial sequence conservation between AChR subtypes, even a small perturbation in structure (that is perhaps too small to be detected even by high resolution x-ray crystallography) can result in a large difference in energy properties. The constants and energies we have measured pertain only to adult-type mouse neuromuscular AChRs and cannot be extrapolated directly to neuronal subtypes.

Nicotine is a high efficacy agonist of adult WT neuromuscular AChRs. This ligand provides ~80% of the binding energy, as does the natural transmitter. However, nicotine is not effective with regard to causing cell depolarization, for two reasons. First, it has a low affinity for resting receptors. $K_d^{nicotine}$ = 1 mM, which is approximately six times higher than for ACh. Second, nicotine is an effective channel blocker. The ratio of the equilibrium dissociation constant for channel block versus binding (K_B/K_d) is one index of the ability of an agonist to depolarize cells. This ratio (at −100 mV) is ~7.2 for ACh but only ~0.7 for nicotine. The equilibrium dissociation constant of nicotine for the AChR pore is about the same as for the transmitter-binding sites, and channel block by nicotine mitigates the cellular response. The amino acids at the transmitter-binding sites and the pore of neuromuscular and neuronal AChRs are similar but not identical. We have not measured ΔG_B, K_B, K_d, and K_B/K_d for nicotine in brain AChRs.

Nornicotine is a minor tobacco alkaloid that is present at a level only ~3% that of nicotine (Jacob et al., 1999). However, the ~50-fold higher affinity and fivefold greater efficacy of nornicotine compared with nicotine suggest that this compound may be more important with regard to its psychoactive properties and smoking than previously considered. Also, $K_d^{nornicotine}$ is only 21 µM, which suggests that its effects, unlike those of nicotine, may not be dulled by channel block.

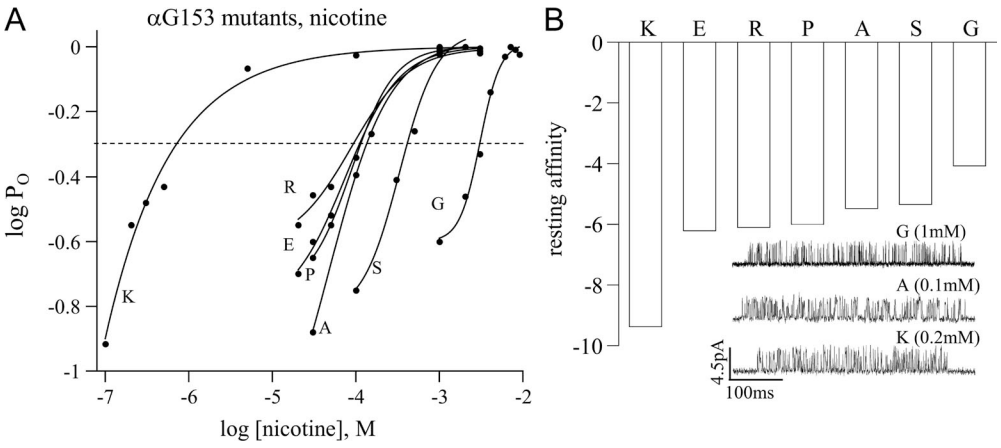

Figure 5. Dose–response curves and K_d values for nicotine in αG153 mutants. (A) Normalized intra-cluster open probability (P_o) as a function of [nicotine]. All mutations decreased EC_{50} (dashed line), with lysine having the largest effect (Table S4). (B; top) Resting affinity for nicotine on a log scale ($-0.59\ln(1/K_d^{nicotine})$). With the lysine, $K_d^{nicotine}$ = 120 nM (Table S6). (Bottom) Example currents in the glycine, alanine, and lysine constructs. Examples of complete cross-concentration fitting are shown in Fig. S2.

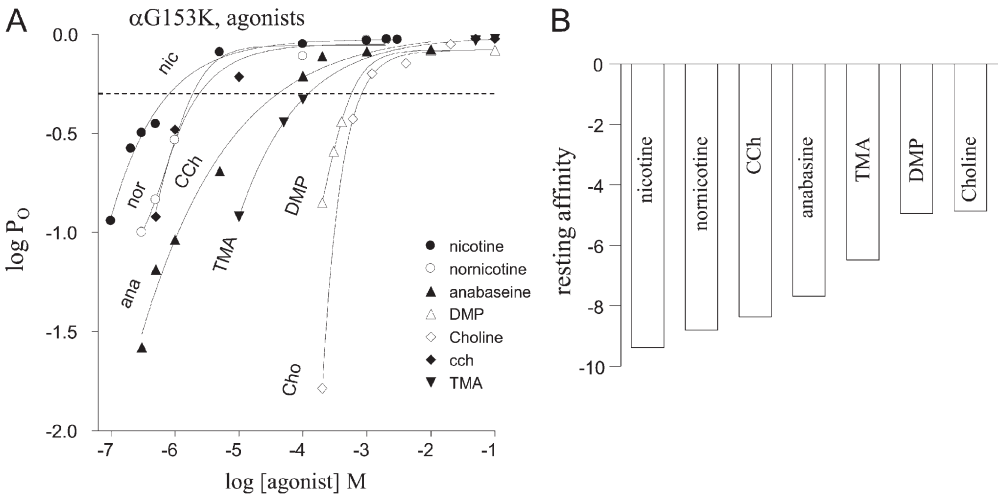

Figure 6. Dose–response curves and activation constants for agonists in αG153K AChRs. (A) The intra-cluster open probability (P_o) as a function of [agonist]. EC_{50} was smallest for nicotine and largest for choline (Table S4). (B) Resting affinity on a log scale ($-0.59\ln(1/K_d)$) (Table S7). The K_d for nicotine is 120 nM, compared with 1 mM in the WT.

αG153 mutants

All of the αG153 mutant–agonist combinations we examined increased activation by increasing both unliganded gating and the resting affinity. The increase in activation with αG153 mutations is quite general. The smallest E_0 value was with glycine, and the largest was with lysine. It appears that these two amino acids at this position have been selected by nature to provide the minimum and maximum activation by physiological ligands.

None of the α153 mutations had a large effect on the agonist affinity ratio. Although αG153 is near αW149, a member of the aromatic triad, this result suggests that it is not part of the binding site apparatus that increases the open probability by increasing the agonist affinity.

All αG153 mutations decreased K_d for all agonists. A comparison of AChBP structures without and with various ligands at the binding site suggests that an inward displacement of loop C occurs in agonist binding (Celie et al., 2004; Hansen et al., 2005; Brams et al., 2011; Shahsavar et al., 2012). Although in *Aplysia* AChBPs there is no discernible displacement of the αG153 backbone between the apo- and ligand-bound structures, the results suggest that in AChRs, loop B also participates in the low affinity–binding rearrangement. As for unliganded gating, glycine and lysine also were the amino acids that fostered the highest and lowest equilibrium constants. This is consistent with the idea that the binding conformational change also occurs in the absence of agonists.

The reduction in K_d was similar for all but one of the mutant/agonist combinations that we examined (~20-fold). The exceptional case was for nicotine plus lysine, which showed a much greater reduction in $K_d^{nicotine}$ compared with the other combinations. That one mutation of one amino acid profoundly increases one activation parameter for one agonist is unusual. The association rate constant for nicotine on αG153K AChRs was $\sim 10^{10}$ $M^{-1}s^{-1}$ (Table S1). Although the geometry and charge of the AChR-binding sites will influence the maximum possible ligand association rate constant, $k_{on}^{nicotine}$ may be close to the upper limit set by diffusion (Berg and von Hippel, 1985). The entry of some agonists into the resting transmitter-binding site has recently been shown to require a conformational change of the protein (Jadey and Auerbach, 2012). The fast association of nicotine in αG153K AChRs indicates that with lysine, this binding conformational change is extremely rapid.

Without structural information is it difficult to infer the molecular forces that determine the fast association of nicotine in αG153K AChRs. It has been suggested that the high resting affinity for nicotine in αG153K AChRs arises from interactions between the lysine and the backbone of loop C at αP197 (Grutter et al., 2003). However, the agonist specificity of the high affinity

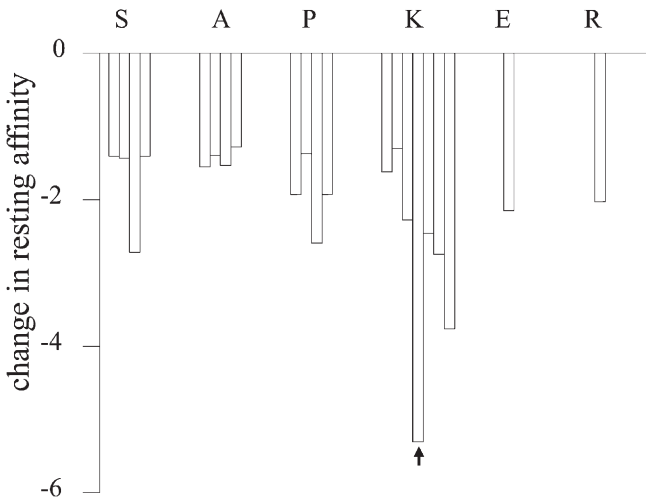

Figure 7. Fold changes in resting affinity in different agonist/αG153 mutant combinations. The energy change of the resting affinity is $-0.59\ln(K_d^{WT}/K_d^{mut})$ (Table S7). All of the agonist mutant combinations showed an increase in the resting affinity (negative energy values). The largest increase was for the αG153K plus nicotine combination (8,130-fold, or −5.3 kcal/mol; arrow). Agonist order for αG153K is (left to right): choline, DMP, TMA, nicotine (arrow), nornicotine, anabasine, and CCh.

phenotype indicates that the ligand, too, is important and is likely involved directly in generating the effect. Our experiments show that methyl pyrrolidine (a fragment of nicotine) and nornicotine do not show the special interaction but that CCh does, to some extent. It has been proposed that the pyridine nitrogen of nicotine makes a cross-subunit hydrogen bond (Blum et al., 2010), so it may be that an interaction of the secondary nitrogen of the agonist is involved in generating fast association in αG153K AChRs.

An experimental association rate is the product of [A] and the association rate constant (k_{on}). It may be that $k_{on}^{nicotine}$ is unusually high in αG153K AChRs, but it is not inconceivable that the lysine induces a rearrangement of the binding site that makes the local [nicotine] (and to some extent CCh) higher than in the bulk extracellular solution. It may be that the long lysine side chain places its ε-amino group near a cluster of charged residues (αK145 and αD200) that have been implicated in starting the agonist-driven opening isomerization (Lee and Sine, 2004; Purohit and Auerbach, 2007). Further experiments are needed to test these speculations.

The exceptionally high affinity for nicotine in αG153K AChRs raises two interesting possibilities. First, it is reasonable to hypothesize that the ancestral tobacco plant synthesized nicotine to target organisms (other than humans) that have a lysine at this position in AChRs. All insects, however, have a glycine at this position and do not respond significantly to nicotine in the nanomolar range (Matsuda et al., 1998). Nicotine is an insecticide, but it will be interesting to ascertain the αG153 side chain in other tobacco pests.

Second, the high affinity for nicotine of αG153K AChRs raises the possibility that mammalian AChRs that have a lysine at this position are exposed to a nicotine-like compound in normal physiology. Aside from its spectacular effect with regard to the resting affinity for nicotine, the functional effects of the lysine substitution are rather pedestrian, yet this amino acid is conserved in many neuronal AChR subtypes. A further exploration of endogenous nicotinoid compounds (for instance, nicotinamide and its metabolites) on K-type AChRs, having a lysine at position αG153, may be informative.

We thank Mary Teeling, Marlene Shero, and Mary Merritt for technical assistance.

This work is supported by National Institutes of Health (grants NS064969 and NS023513).

Edward N. Pugh Jr. served as editor.

Submitted: 13 September 2012
Accepted: 10 December 2012

REFERENCES

Akk, G., and A. Auerbach. 1999. Activation of muscle nicotinic acetylcholine receptor channels by nicotinic and muscarinic agonists. *Br. J. Pharmacol.* 128:1467–1476. http://dx.doi.org/10.1038/sj.bjp.0702941

Auerbach, A. 2012. Thinking in cycles: MWC is a good model for acetylcholine receptor-channels. *J. Physiol.* 590:93–98.

Berg, O.G., and P.H. von Hippel. 1985. Diffusion-controlled macromolecular interactions. *Annu. Rev. Biophys. Biophys. Chem.* 14:131–160. http://dx.doi.org/10.1146/annurev.bb.14.060185.001023

Blum, A.P., H.A. Lester, and D.A. Dougherty. 2010. Nicotinic pharmacophore: the pyridine N of nicotine and carbonyl of acetylcholine hydrogen bond across a subunit interface to a backbone NH. *Proc. Natl. Acad. Sci. USA.* 107:13206–13211. http://dx.doi.org/10.1073/pnas.1007140107

Brams, M., A. Pandya, D. Kuzmin, R. van Elk, L. Krijnen, J.L. Yakel, V. Tsetlin, A.B. Smit, and C. Ulens. 2011. A structural and mutagenic blueprint for molecular recognition of strychnine and *d*-tubocurarine by different cys-loop receptors. *PLoS Biol.* 9:e1001034. http://dx.doi.org/10.1371/journal.pbio.1001034

Brejc, K., W.J. van Dijk, R.V. Klaassen, M. Schuurmans, J. van Der Oost, A.B. Smit, and T.K. Sixma. 2001. Crystal structure of an ACh-binding protein reveals the ligand-binding domain of nicotinic receptors. *Nature.* 411:269–276. http://dx.doi.org/10.1038/35077011

Celie, P.H., S.E. van Rossum-Fikkert, W.J. van Dijk, K. Brejc, A.B. Smit, and T.K. Sixma. 2004. Nicotine and carbamylcholine binding to nicotinic acetylcholine receptors as studied in AChBP crystal structures. *Neuron.* 41:907–914. http://dx.doi.org/10.1016/S0896-6273(04)00115-1

Changeux, J., and S.J. Edelstein. 2001. Allosteric mechanisms in normal and pathological nicotinic acetylcholine receptors. *Curr. Opin. Neurobiol.* 11:369–377. http://dx.doi.org/10.1016/S0959-4388(00)00221-X

Chavez-Noriega, L.E., J.H. Crona, M.S. Washburn, A. Urrutia, K.J. Elliott, and E.C. Johnson. 1997. Pharmacological characterization of recombinant human neuronal nicotinic acetylcholine receptors hα2β2, hα2β4, hα3β2, hα3β4, hα4β2, hα4β4 and hα7 expressed in *Xenopus* oocytes. *J. Pharmacol. Exp. Ther.* 280:346–356.

Connolly, J., J. Boulter, and S.F. Heinemann. 1992. α4-β2 and other nicotinic acetylcholine receptor subtypes as targets of psychoactive and addictive drugs. *Br. J. Pharmacol.* 105:657–666. http://dx.doi.org/10.1111/j.1476-5381.1992.tb09035.x

Corringer, P.J., S. Bertrand, S. Bohler, S.J. Edelstein, J.P. Changeux, and D. Bertrand. 1998. Critical elements determining diversity in agonist binding and desensitization of neuronal nicotinic acetylcholine receptors. *J. Neurosci.* 18:648–657.

Gotti, C., D. Fornasari, and F. Clementi. 1997. Human neuronal nicotinic receptors. *Prog. Neurobiol.* 53:199–237. http://dx.doi.org/10.1016/S0301-0082(97)00034-8

Gotti, C., M. Zoli, and F. Clementi. 2006. Brain nicotinic acetylcholine receptors: native subtypes and their relevance. *Trends Pharmacol. Sci.* 27:482–491. http://dx.doi.org/10.1016/j.tips.2006.07.004

Grutter, T., L. Prado de Carvalho, N. Le Novère, P.J. Corringer, S. Edelstein, and J.P. Changeux. 2003. An H-bond between two residues from different loops of the acetylcholine binding site contributes to the activation mechanism of nicotinic receptors. *EMBO J.* 22:1990–2003. http://dx.doi.org/10.1093/emboj/cdg197

Gupta, S., and A. Auerbach. 2011. Temperature dependence of acetylcholine receptor channels activated by different agonists. *Biophys. J.* 100:895–903. http://dx.doi.org/10.1016/j.bpj.2010.12.3727

Hansen, S.B., G. Sulzenbacher, T. Huxford, P. Marchot, P. Taylor, and Y. Bourne. 2005. Structures of Aplysia AChBP complexes with nicotinic agonists and antagonists reveal distinctive binding interfaces and conformations. *EMBO J.* 24:3635–3646. http://dx.doi.org/10.1038/sj.emboj.7600828

Jacob, P., III, L. Yu, A.T. Shulgin, and N.L. Benowitz. 1999. Minor tobacco alkaloids as biomarkers for tobacco use: comparison of users of cigarettes, smokeless tobacco, cigars, and pipes. *Am. J. Public Health.* 89:731–736. http://dx.doi.org/10.2105/AJPH.89.5.731

Jadey, S., and A. Auerbach. 2012. An integrated catch-and-hold mechanism activates nicotinic acetylcholine receptors. *J. Gen. Physiol.* 140:17–28. http://dx.doi.org/10.1085/jgp.201210801

Jadey, S.V., P. Purohit, I. Bruhova, T.M. Gregg, and A. Auerbach. 2011. Design and control of acetylcholine receptor conformational change. *Proc. Natl. Acad. Sci. USA.* 108:4328–4333. http://dx.doi.org/10.1073/pnas.1016617108

Jensen, A.A., B. Frølund, T. Liljefors, and P. Krogsgaard-Larsen. 2005. Neuronal nicotinic acetylcholine receptors: structural revelations, target identifications, and therapeutic inspirations. *J. Med. Chem.* 48:4705–4745. http://dx.doi.org/10.1021/jm040219e

Jha, A., and A. Auerbach. 2010. Acetylcholine receptor channels activated by a single agonist molecule. *Biophys. J.* 98:1840–1846. http://dx.doi.org/10.1016/j.bpj.2010.01.025

Jha, A., P. Purohit, and A. Auerbach. 2009. Energy and structure of the M2 helix in acetylcholine receptor-channel gating. *Biophys. J.* 96:4075–4084. http://dx.doi.org/10.1016/j.bpj.2009.02.030

Karlin, A. 1967. On the application of "a plausible model" of allosteric proteins to the receptor for acetylcholine. *J. Theor. Biol.* 16:306–320. http://dx.doi.org/10.1016/0022-5193(67)90011-2

Kem, W.R., V.M. Mahnir, R.L. Papke, and C.J. Lingle. 1997. Anabaseine is a potent agonist on muscle and neuronal alpha-bungarotoxin-sensitive nicotinic receptors. *J. Pharmacol. Exp. Ther.* 283:979–992.

Lee, W.Y., and S.M. Sine. 2004. Invariant aspartic acid in muscle nicotinic receptor contributes selectively to the kinetics of agonist binding. *J. Gen. Physiol.* 124:555–567. http://dx.doi.org/10.1085/jgp.200409077

Lindstrom, J. 1997. Nicotinic acetylcholine receptors in health and disease. *Mol. Neurobiol.* 15:193–222. http://dx.doi.org/10.1007/BF02740634

Matsuda, K., S.D. Buckingham, J.C. Freeman, M.D. Squire, H.A. Baylis, and D.B. Sattelle. 1998. Effects of the alpha subunit on imidacloprid sensitivity of recombinant nicotinic acetylcholine receptors. *Br. J. Pharmacol.* 123:518–524. http://dx.doi.org/10.1038/sj.bjp.0701618

Mitra, A., T.D. Bailey, and A.L. Auerbach. 2004. Structural dynamics of the M4 transmembrane segment during acetylcholine receptor gating. *Structure.* 12:1909–1918. http://dx.doi.org/10.1016/j.str.2004.08.004

Monod, J., J. Wyman, and J.P. Changeux. 1965. On the nature of allosteric transitions: a plausible model. *J. Mol. Biol.* 12:88–118. http://dx.doi.org/10.1016/S0022-2836(65)80285-6

Nayak, T.K., P.G. Purohit, and A. Auerbach. 2012. The intrinsic energy of the gating isomerization of a neuromuscular acetylcholine receptor channel. *J. Gen. Physiol.* 139:349–358. http://dx.doi.org/10.1085/jgp.201110752

Papke, R.L., L.P. Dwoskin, and P.A. Crooks. 2007. The pharmacological activity of nicotine and nornicotine on nAChRs subtypes: relevance to nicotine dependence and drug discovery. *J. Neurochem.* 101:160–167. http://dx.doi.org/10.1111/j.1471-4159.2006.04355.x

Purohit, P., and A. Auerbach. 2007. Acetylcholine receptor gating: Movement in the α-subunit extracellular domain. *J. Gen. Physiol.* 130:569–579. http://dx.doi.org/10.1085/jgp.200709858

Purohit, P., and A. Auerbach. 2009. Unliganded gating of acetylcholine receptor channels. *Proc. Natl. Acad. Sci. USA.* 106:115–120. http://dx.doi.org/10.1073/pnas.0809272106

Purohit, P., and A. Auerbach. 2011. Glycine hinges with opposing actions at the acetylcholine receptor-channel transmitter binding site. *Mol. Pharmacol.* 79:351–359. http://dx.doi.org/10.1124/mol.110.068767

Purohit, P., I. Bruhova, and A. Auerbach. 2012. Sources of energy for gating by neurotransmitters in acetylcholine receptor channels. *Proc. Natl. Acad. Sci. USA.* 109:9384–9389. http://dx.doi.org/10.1073/pnas.1203633109

Rucktooa, P., A.B. Smit, and T.K. Sixma. 2009. Insight in nAChR subtype selectivity from AChBP crystal structures. *Biochem. Pharmacol.* 78:777–787. http://dx.doi.org/10.1016/j.bcp.2009.06.098

Shahsavar, A., J.S. Kastrup, E.O. Nielsen, J.L. Kristensen, M. Gajhede, and T. Balle. 2012. Crystal structure of *Lymnaea stagnalis* AChBP complexed with the potent nAChR antagonist DHβE suggests a unique mode of antagonism. *PLoS ONE.* 7:e40757. http://dx.doi.org/10.1371/journal.pone.0040757

Sine, S.M., K. Ohno, C. Bouzat, A. Auerbach, M. Milone, J.N. Pruitt, and A.G. Engel. 1995. Mutation of the acetylcholine receptor α subunit causes a slow-channel myasthenic syndrome by enhancing agonist binding affinity. *Neuron.* 15:229–239. http://dx.doi.org/10.1016/0896-6273(95)90080-2

Unwin, N. 2005. Refined structure of the nicotinic acetylcholine receptor at 4A resolution. *J. Mol. Biol.* 346:967–989. http://dx.doi.org/10.1016/j.jmb.2004.12.031

Xiu, X., N.L. Puskar, J.A. Shanata, H.A. Lester, and D.A. Dougherty. 2009. Nicotine binding to brain receptors requires a strong cation-pi interaction. *Nature.* 458:534–537. http://dx.doi.org/10.1038/nature07768

Zhou, M., A.G. Engel, and A. Auerbach. 1999. Serum choline activates mutant acetylcholine receptors that cause slow channel congenital myasthenic syndromes. *Proc. Natl. Acad. Sci. USA.* 96:10466–10471. http://dx.doi.org/10.1073/pnas.96.18.10466